

Elektronik

Simon Delchambre

**Linear Momentum Enhancement
Beta-Factor Estimation Technique for
Asteroid Deflection Missions**

**SHAKER
VERLAG**



**Schätzverfahren des Linearen
Beta-Impulsverstärkungsfaktors für
Asteroiden-Ablenkungsmissionen**

Linear Momentum Enhancement Beta-Factor Estimation
Technique for Asteroid Deflection Missions

Simon Delchambre

von der Fakultät Elektrotechnik und Informationstechnik
der Technischen Universität Dresden

zur Erlangung des akademischen Grades eines
Doktorandenieurs
(Dr.-Ing.)

genehmigte Dissertation

———— * ———

Vorsitzender: Prof. Dr.-Ing. Dirk Plettemeier

Gutachter: Prof. Dr. techn. Klaus Janschek
Prof. Dr. A. Fitzsimmons

Tag der Einreichung: 28.02.2018

Tag der Verteidigung: 04.12.2018

Berichte aus der Elektronik

Simon Delchambre

**Linear Momentum Enhancement Beta-Factor
Estimation Technique for Asteroid Deflection Missions**

Shaker Verlag
Aachen 2019

Bibliographic information published by the Deutsche Nationalbibliothek

The Deutsche Nationalbibliothek lists this publication in the Deutsche Nationalbibliografie; detailed bibliographic data are available in the Internet at <http://dnb.d-nb.de>.

Zugl.: Dresden, Techn. Univ., Diss., 2018

Copyright Shaker Verlag 2019

All rights reserved. No part of this publication may be reproduced, stored in a retrieval system, or transmitted, in any form or by any means, electronic, mechanical, photocopying, recording or otherwise, without the prior permission of the publishers.

Printed in Germany.

ISBN 978-3-8440-6590-9

ISSN 1436-3801

Shaker Verlag GmbH • P.O. BOX 101818 • D-52018 Aachen

Phone: 0049/2407/9596-0 • Telefax: 0049/2407/9596-9

Internet: www.shaker.de • e-mail: info@shaker.de

Acknowledgements

Foremost, I would like to express my sincere gratitude to my advisor Univ.-Prof. Dr. techn. Klaus Janschek for his support, motivation and guidance since the very first day of this research. It was an honor to receive feedback and insightful advice from his side. Further, I have to thank genuinely Dipl.-Ing. Tobias Ziegler for his daily, if not hourly support in the last three years and the enthusiasm he brings along in tackling new problems. Not only his academic support, also the countless bike rides and the many wonderful opportunities in- and outside the company I got are memorable.

I am also grateful to all of the colleagues and friends with whom I have had the pleasure to work during this and other related projects at Airbus in Friedrichshafen. Each of them has provided me extensive personal and professional guidance and taught me a great deal about both scientific research and industrial projects. I would especially like to thank Albert, Alex, Nico, Stefan, Tom, Uwe for the advice, care and interest they have shown in the last three years.

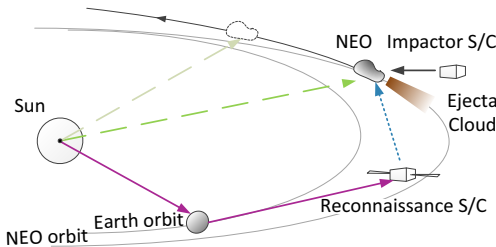
Nobody has been more important to me in the pursuit of this degree than the members of my family. I would like to thank my parents, brother, grandparents, uncles, aunts and cousins. They are unique in many ways and motivated me till the very last day. Most importantly, I wish to thank my loving and supportive future wife, Carina, who provided endless advice, patience and inspiration.

This work is a milestone in my academic career which ends a long journey through Belgium, Sweden, France and Germany. I was lucky to have met so many interesting personalities with whom I shared joy and excitement.

This work would not have been possible without the financial support of the Airbus Research and Development program. I am especially indebted to Dr. Georg Willich, Head of Research and Development, who has given me the opportunity and support with advice and the protected academic time to pursue those goals.

Kurzfassung

[Problembeschreibung] Missionen, die die Ablenkung eines Near-Earth Object (NEO) durch einen kinetischen Impaktor demonstrieren, stoßen in der *Planetary Defense Community* auf steigendes Interesse, um die Herausforderungen und die Dynamik von Einschlagszenarien besser verstehen zu können. Von besonderem Interesse ist hierbei der β -Faktor, der die Impulsverstärkung beschreibt, die durch die Energie der ausgeworfenen Materiewolke nach Einschlag entsteht. Die Prädiktion dieses β -Faktors wurde in der Literatur im letzten Jahrzehnt ausführlich behandelt, die Schätzverfahren dazu wurden bisher jedoch nicht untersucht. **[Methodik]** Zunächst liefert diese Arbeit zwei Definitionen des eindeutigen β -Faktors, die beide die Gleichung des Erhaltungssatzes für den linearen Impuls sowie den Drehimpuls lösen. Um den Impulsverstärkungsfaktors genauer schätzen zu können, wird im zweiten Teil der Arbeit eine robuste Beobachtungsstrategie entwickelt. Im dritten Schritt wird mithilfe des Aufklärungssatelliten S/C ein Schätzverfahren zur Bestimmung der heliozentrischen Bahn kleiner NEOs entwickelt, bei dem Radio Science Ortungsdaten mit der Information aus der optischen Navigation fusioniert werden. Abschließend werden die Ergebnisse aus der Bahnbestimmung zur Schätzung des β -Faktors und des Fehlerbudgets herangezogen.

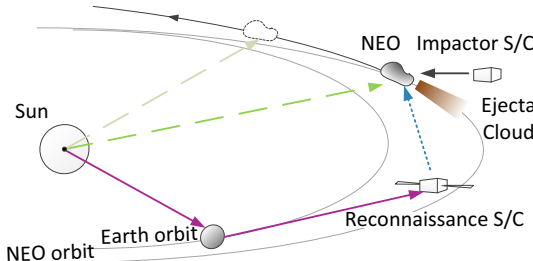


[Ergebnisse] Die Güte der Schätzung hängt stark von den relativen Navigationsgenauigkeiten und der Verfügbarkeit der Bodenstationen ab. Die numerische Auswertung des Referenzszenarios bestätigt, dass der β -Faktor nach einer 14-tägigen Beobachtungszeit bei 67% Verfügbarkeit der ESA Verfolgungsstationen und mit einem Manöver zur Bahnerhaltung des Aufklärungssatelliten pro Tag mit einer Genauigkeit von 2% (1σ), was geschätzt werden kann. **[Fazit]** Diese Güte der Schätzung trägt in einem sehr kurzen Zeitrahmen zu einer wesentlichen Reduzierung der Unsicherheit des β -Faktors bei und ist robust gegenüber großen Unsicherheiten, die aus der unbekannten Impulsverstärkung der Auswurfwolke resultieren.

Abstract

[Background and Problem] A near-Earth Object (NEO) kinetic impactor demonstration mission is gaining interest among the planetary defense community to better understand the challenges and the dynamics of an impact scenario. Of particular interest is the β -factor that expresses the momentum gain caused by ejecta cloud dynamics after impact. Prediction of the β -factor has been addressed extensively in the literature over the last decade, estimation techniques have not been investigated so far.

[Methods] First, this work presents two unambiguous β -factor definitions for the linear and angular momentum conservation equation. Second, a robust observation strategy is developed for the Reconnaissance S/C at the close proximity of the NEO to support the momentum enhancement factor estimation. Third, a NEO heliocentric orbit determination estimator for small NEOs is setup with the support of a Reconnaissance S/C where radioscience tracking data is fused with optical navigation information. Last, the orbit determination results are used to estimate the β -factor and to establish an error budget.



[Results] The estimation performance largely depends on the relative navigation accuracies and the ground station availabilities. Numerical evaluation confirms for the reference scenario a β -factor estimation accuracy of 2% (1σ) after 14 days of monitoring with 67% availability of the ESA tracking stations and one Reconnaissance S/C station-keeping manoeuvre per day. Extending the monitoring window to 28 days only improves the estimation accuracy fractionally. **[Conclusions]** This estimation performance considerably reduces the β -factor uncertainty in a very short time frame and is robust to large uncertainties in the ejecta cloud momentum gain and direction.

Contents

Kurzfassung	v
Abstract	vii
Contents	ix
Nomenclature	xvii
1 Introduction	1
1.1 Threat of Small Near-Earth Objects	1
1.2 Near-Earth Object Impact Techniques	3
1.3 Small Body Impact Studies and Missions	5
2 Research Outline	9
2.1 Research Motivation	9
2.2 Research Assumptions	9
2.3 State-of-the-Art and Research Contributions	14
2.4 Research Methodology and Structure	20
3 Momentum Enhancement Factor	21
3.1 Current Definitions	21
3.2 Definition Extension	25
3.2.1 Shortcomings of the Current Definitions	26
3.2.2 Generalized Definitions	26
3.3 Summary	35
4 State Estimation Technique Trade-off	37
4.1 Stochastic Variables and Gaussian Distribution	37
4.2 Least Square and Minimum Variance Estimation	42
4.3 Discrete-Time Kalman Filter	46
4.3.1 The Algorithm	46
4.3.2 Extended Kalman Filter	50
4.3.3 Consider Extended Kalman Filter	51
4.4 Batch State Estimation	53
4.5 Consistency of the Estimation Filter	53
4.6 Summary	54
5 Near-Earth Object Orbit Determination	57
5.1 Near-Earth Object Orbit Determination Concept	57

Contents

5.2	Reconnaissance S/C Absolute Orbit Determination	58
5.2.1	Dynamics	59
5.2.2	Observations	61
5.2.3	Filter Model	64
5.3	Reconnaissance S/C Relative Orbit Determination	65
5.3.1	Dynamics	65
5.3.2	Observations	68
5.3.3	Filter Model	75
5.4	Near-Earth Object Absolute Orbit Determination	76
5.4.1	Dynamics	76
5.4.2	Observations	80
5.4.3	Filter Model	94
5.5	Summary	95
6	Momentum Enhancement Factor Estimation	97
6.1	Estimation Methodology	97
6.2	Estimation Error Budget	103
6.3	Summary	107
7	Case Study: Mitigating NEO 2001 QC34	111
7.1	Scenario Overview	111
7.2	Scenario Results	114
Conclusions and Future Work		127
Appendix A NEO Characterization Performance		133
Appendix B Case Study: Filter Parametrization		135
Appendix C Filter Routines		139
Appendix D Publications		143
Appendix E Curriculum Vitae		145
References		147

List of Figures

1.1	Asteroid sizes shown up to scale	2
1.2	Predicted near-Earth asteroid population and discovery rate.	3
1.3	Aproximate outline of the regimes of primary applicability of the four types of mitigation in function of warning time and diameter	6
2.1	The setup of the research problem. A Reconnaissance S/C is part of the mission design and hovers at the close-proximity of the NEO. The distance between the NEO and the Sun is varying around 1 AU, the distance between the Reconnaissance S/C and NEO is controlled to about 5 km. The illustration is not up to scale.	10
2.2	Three-dimensional shape model views of Lutetia from low northern latitude at different longitudes. Images taken with the OSIRIS NAC camera were used.	12
2.3	Three-dimensional final SPG SHAP4S shape model views of 67P/Churyumov-Gerasimenko from different latitudes. Images taken with the OSIRIS NAC camera were used	13
2.4	This diagram shows the three current momentum enhancement factor research domains and identifies the contributions of this work to the state-of-the-art literature. The four contributions of this work are marked correspondingly C1-C4.	19
3.1	The impact scenario with the ejecta momentum vector p_{ej} along but backwards to the Impactor S/C velocity vector mU , as assumed by Housen and Holsapple.	24
3.2	The impact scenario with the ejecta momentum vector p_{ej} along but backwards to the local normal \mathbf{n} at impact point A, as assumed by Scheeres.	25
3.3	In-plane geometrical setup of impact with relative spacecraft momentum, relative net ejecta momentum and resulting relative NEO momentum change. All quantities are relative to the NEO center of mass O at impact.	27
3.4	Four momentum enhancement scenarios with different directions for the ejecta plume for which the various β -values have been calculated. The results are presented in Table 3.1	33
4.1	Illustration of a deterministic signal $y_{det}(t) = \cos \pi t + 5e^{-3t}$ and the stochastic signal $y_{st}(t) = \cos \pi t + 5e^{-3t} + w$	38

4.2	Probability density function $X \sim \mathcal{N}(13, 1)$	40
4.3	Estimation method trade-off for the S/C absolute and relative orbit determination filter that will use the Discrete Time Consider Extended Kalman Filter. The NEO absolute orbit determination filter wil additionally use the RTS smoother to further decrease the orbit uncertainties.	56
5.1	Near-Earth Object orbit determination concept. The orbit of the NEO is retrieved over the SSB-Reconnaissance S/C-NEO links.	58
5.2	Minimum Reconnaissance S/C semimajor axes that ensure escape of the NEO environment due to high SRP-gravity ratios.	68
5.3	Free fall trajectories from initial altitude of 1 and 5km, starting with initial velocities 0, 2 and 5cm/s. The SRP is assumed to act parallel to the NEO gravity and thus accelerates the free fall.	69
5.4	Near-inertial hovering concept illustration.	69
5.5	Relative orbit determination concept.	70
5.6	Pose estimation functional architecture. The features of the images are matched with the landmarks of the database by the feature matching algorithm. The iterative Point-to-point pose estimation algorithm calculates the relative position and altitude of the Reconnaissance S/C relative to the NEO.	73
5.7	Average pose estimation errors (distance u , attitude θ and pixel error u) using SSD matching (left) where a RANSAC filter (center) and an additional pixel filter (right) detect and remove the erroneous matches. The RANSAC and pixel filter result in more accurate pose estimations for a high tolerance level.	74
5.8	Landmark-feature matches between image and database (overlaid in blue) after SSD matching (left) where a RANSAC filter (center) and an additional pixel filter (right) remove the 6 erroneous matches (marked red).	74
5.9	Schematic representation of the Yarkovsky effect. A force, resulting from the thermal radiation, increases the semimajor axis for prograde rotators.	79

5.10 Reconnaissance S/C absolute state estimation error. The update epochs by the Delta-DOR measurements are marked with a red cross (1/day). Results of the case study in Chapter 7 have been used for illustrative purposes.	85
5.11 Right: Principle of the NEO pseudo range measurement R_{neo} . The Earth - Reconnaissance S/C range measurement R_{sc} is shifted onto the NEO center of mass, using the relative orbit state estimation. Left: The error budget is composed of the range linearization error (red), the error due to the false linearization point (purple), the S/C range measurement error (green) and the relative orbit estimation error (blue). The two tangents are the range sensitivities evaluated at the true spacecraft position (1) and the estimated spacecraft position (2). Maximum errors for these four components are summarized in Table 5.3.	91
5.12 Left: Radioscience residuals for Reconnaissance S/C. Errors are defined as true measurements minus the ideal measurements. Right: Pseudo radioscience residuals for NEO driven by the Reconnaissance S/C residuals and the relative navigation results. Results of the case study in Chapter 7 have been used for illustrative purposes.	92
5.13 Reconnaissance S/C relative state estimation errors. Errors are defined as true measurements minus expected. Results of the case study in Chapter 7 have been used for illustrative purposes.	93
5.14 NEO orbit determination routine with the three CEKF subroutines: Absolute Reconnaissance S/C CEKF (purple), Relative Reconnaissance S/C CEKF (blue), Absolute NEO FIS with the CEKF-RTS (green).	96
6.1 Linear momentum enhancement factor breakdown tree. . .	99
6.2 NEO orbit uncertainties over time after the forward CEKF and backward RTS operation. The drawing is only for an illustrative purpose.	100
6.3 NEO Pseudo doppler minus the expected Doppler from the NEO absolute orbit determination filter. The unmodeled and unknown delta-v causes a drop in the signal due to the unmodeled deceleration of the NEO. Results of the case study in Section 7 have been used for illustrative purposes.	104

6.4 NEO Absolute velocity estimation error with 3σ covariance boundary. Due to the large momentum enhancement effect of the ejecta, the filter is shortly inconsistent. Results of the case study in Section 7 have been used for illustrative purposes.	105
7.1 Spacecraft and ejecta momentum acting on 2001 QC34 for the reference scenario. The momentum enhancement factor is 5 and the angle between the two momenta is 15°	112
7.2 The hovering motion of the Reconnaissance S/C above the NEO.	115
7.3 Reconnaissance S/C absolute orbit CEKF estimation errors in the inertial frame. The impact occurs at $t_1=7$ days. Errors are defined as the true minus the estimated value.	117
7.4 Reconnaissance S/C pose measurements and errors.	119
7.5 Reconnaissance S/C relative orbit CEKF estimation errors in the inertial frame. The impact occurs at $t_1=7$ days. Errors are defined as the true minus the estimated value.	120
7.6 NEO absolute velocity estimation errors after the forward step (CEKF) and the smoothing (RTS). Errors are defined as true velocity minus estimated. The impact occurs at $t_1=7$ days, which means a pre-impact monitoring time of one week.	121
7.7 Reconnaissance S/C and NEO absolute orbit measurements.	122
7.8 NEES Error statistic for the three estimation routines. The minimum and maximum values indicate the NEES regions for consistent filters.	124
7.9 Beta gain error for 50 Monte Carlo runs. All errors are within the expected 3σ boundary.	125

List of Tables

1.1	Predicted NEA average impact interval and possible consequences. Small NEA ($d < 300\text{m}$) impacts can have catastrophic consequences already.	4
3.1	The β -values results for the scenarios presented in Figure 3.4	34
4.1	Trade-off for filter architectures for dynamic systems. The selected filter for the NEO absolute orbit determination problem is marked green.	55
5.1	Typical acceleration order of magnitudes for Reconnaissance S/C operating at 5 km distance from the NEO. A ballistic coefficient of 24 kg/m^2 and 20 N thrusters were assumed.	71
5.2	NEO Semimajor axis uncertainties.	80
5.3	Budget error composition for the NEO pseudo radioscience measurements assuming maximum absolute orbit estimation errors of 10km and 10m/s (3σ) and relative orbit estimation errors of 10m and 1 mm/s (3σ).	90
6.1	Budget error share for different nominal delta-v's ($r=1\dots10$). The contributions are expressed as an absolute and relative (in percentage) value after 7 days of pre- and 7 days of post impact monitoring. Relative values are expressed in percentage of the total error $\sigma_{\beta lin}^2$. The results of Chapter 7 are used for illustrative purposes.	108
6.2	Budget error share for different nominal delta-v's ($r=1\dots10$). The contributions are expressed as an absolute and relative (in percentage) value after 14 days of pre- and 14 days of post impact monitoring. Relative values are expressed in percentage of the total error $\sigma_{\beta lin}^2$. The results of Chapter 7 are used for illustrative purposes.	109
7.1	NEOShield-2 Kinetic Impact Scenario overview.	113
7.2	NEOShield-2 KI scenario estimation results. (*) Value has not been actively estimated in this work.	126
A.1	SPG characterisation performance indices for Lutetia and 67P/Churyumov-Gerasimenko and the extrapolated performance assumed for the NEO 2001 QC34 used in this work.	133

B.1	Filter paramatrisation for all three estimation routines used for the reference scenario presented in Chapter 7.	137
C.1	Kalman filter routine equations for a discrete-discrete model.	139
C.2	Extended Kalman filter routine equations for continuous- discrete model.	140
C.3	Consider Extended Kalman Filter routine equations for continuous- discrete model.	141
C.4	RTS smoother equations for continuous-discrete model. . .	142

Nomenclature

Acronyms

AIDA	Asteroid Impact and Deflection Assessment
AIM	Asteroid Impact Mission
AOCS	Attitude and Orbital Control Systems
BD	Blast Deflection
CEKF	Consider Extended Kalman Filter
CKF	Consider Kalman Filter
CoM	Center of Mass
DART	Double Asteroid Redirect Test
DCM	Direct Cosine Matrix
Delta-	Delta-Differential One-way Ranging
DOF	
EC	European Commission
EKF	Extended Kalman Filter
ESA	European Space Agency
ESOC	European Space Operations Centre
FIS	Fixed Interval Smoother
GNC	Guidance, Navigation and Control
ISAS	Institute of Space and Astronautical Science
JAXA	Japan Aerospace Exploration Agency
JPL	Jet Propulsion Laboratory
KI	Kinetic Impactor
NASA	National Aeronautics and Space Administration
NEA	Near-Earth Asteroid
NEC	Near-Earth Comet
NEES	Normalized Estimation Error Squared
NEO	Near-Earth Object
NRC	National Research Council
PDF	Probability Density Function
PHA	Potentially Hazardous Asteroid
RSE	Radio Science Experiment
RTS	Rauch, Tung, and Striebel Smoother
S/C	Spacecraft
SKM	Station Keeping Manoeuvre
SPA	Solar Phase Angle
SPG	Stereo-photogrammetry
SRIF	Square Root Information Filter

SRP	Solar Radiation Pressure
SSB	Solar System Barycenter
TRL	Technology Readiness Level

Vector notation

$\mathbf{r}_{[to]}^{[ref], [from]}$ = Position vector from [from] to [to],

expressed in reference frame [ref].

$$= [\mathbf{r}_{[to]}^{[ref], [from]}(x) \quad \mathbf{r}_{[to]}^{[ref], [from]}(y) \quad \mathbf{r}_{[to]}^{[ref], [from]}(z)] \quad (1)$$

If [from] would be the origin of the reference frame, it will be omitted as: $\mathbf{r}_{[to]}^{[ref]}$. If [ref] is a latin letter (e.g. J , it refers to a 3D-reference system. In case of a greek letter (e.g. π), a 3D-projection onto the 2D-plane is meant.

Latin Symbols

Symbol	Description	Units	Dim.
a	Semimajor axis	m	1
A_{sc}	Spacecraft cross surface exposed to solar radiation	m^2	1
B_{sc}	Spacecraft ballistic coefficient	$kg \cdot m^2$	1
c	Speed of light	m/s	1
c_{Rs}^i	Specular reflection coeff. of surface A_i	-	1
c_{Rd}^i	Diffusive reflection coeff. of surface A_i	-	1
c_{Ra}^i	Absorption coefficient of coeff. surface A_i	-	1
\mathbf{e}_i	Unit vector in the direction i	-	3×1
\mathbf{e}	Residual error between predicted and true measurement i	-	$m \times 1$
E	Energy	J	1
E_k	Kinetic energy	J	1
E_i	Internal energy	J	1

E_c	Communition energy	J	1
E_h	Internal heat energy	J	1
E_m	Elastic wave and other internal energies	J	1
f_x	Probability density function i	-	1
J_{ls}	Least square cost function	dep.	1
J_{mv}	Minimum variance cost function	dep.	1
J_{wls}	Weighted least square cost function	dep.	1
H	Measurement matrix	dep.	$m \times n$
${}_{sc}^{\pi}K$	Intrinsic camera matrix		3×4
n	State size (index)	-	-
m	Measurement size (index)	-	-
m_{imp}	Impactor S/C Mass	kg	1
m_{sc}	Reconnaissance S/C mass	kg	1
M	NEO Mass	kg	1
${}^J\mathbf{n}_i$	Normal of surface A_i expressed in frame $\{J\}$	-	3×1
${}^J\mathbf{p}_{ej}$	Ejecta momentum expressed in frame $\{J\}$	kg/m/s	3×1
${}^J\mathbf{p}_{sc}^{neo}$	Spacecraft pose relative to the NEO	$3 \times m$ $4 \times [-]$	7×1
P_{\odot}	Solar Constant	$\mu N/m^2$	1
P	Covariance Matrix	dep.	$n \times n$
P^-	A priori state covariance matrix	dep.	$n \times 1$
P^+	A posterioricovariance matrix	dep.	$n \times 1$
${}^{[ref]} \mathbf{r}_{[tol]}^{[from]}$	Position vector from [from] to [to], expressed in reference reference frame [ref]	m	3×1
R	Measurement noise matrix	dep	$m \times m$
$R_{\beta,lin}$	Linear momentum enhancement DCM	-	3×3
$R_{\beta,ang}$	Angular momentum enhancement DCM	-	3×3
${}^J\mathbf{s}_i$	Sun direction expressed in frame $\{J\}$	-	3×1
${}^J\mathbf{U}$	Impactor S/C relative velocity expressed in frame $\{J\}$	m/s	3×1
Q	Process noise matrix	dep.	$n \times n$
${}^{\pi}u$	Feature u-coordinate in image plane $\{\pi\}$	pixel	1
${}^{\pi}v$	Fature y-coordinate in image plane $\{\pi\}$	pixel	1
\mathbf{v}	Process noise	dep.	$n \times 1$
\mathbf{w}	Measurement noise	dep.	$m \times 1$
\mathbf{x}	True State	dep.	$n \times 1$
$\hat{\mathbf{x}}^-$	Priori state estimate	dep.	$n \times 1$
$\hat{\mathbf{x}}^+$	Posteriori state estimate	dep.	$n \times 1$

$\tilde{\mathbf{x}}^-$	Prior state estimate error	dep.	$n \times 1$
$\tilde{\mathbf{x}}^+$	Posteriori state estimate error	dep.	$n \times 1$
$\bar{\mathbf{x}}(t)$	Nominal state	dep.	$n \times 1$
X_{neo}	NEO Landmark x-coordinate	m	3×1
\mathbf{y}	Theoretical measurements	-	$m \times 1$
$\tilde{\mathbf{y}}$	True (noisy) measurements	dep.	$m \times 1$
$\hat{\mathbf{y}}$	Estimated/Predicted measurement	dep.	$m \times 1$

Greek Symbols

Symbol	Description	Units	Dim.
β	Linear enhancement factor	dep.	1
β_{hh}	Linear enhancement factor, defined by Housen and Holsapple	-	1
β_{sc}	Linear enhancement factor, defined by Scheeres	-	1
β_{lin}	Linear enhancement factor	-	3×3
β_{ang}	Angular enhancement factor	-	3×3
β_{lin}	Linear enhancement gain	-	1
β_{ang}	Angular enhancement gain	-	1
Δ	Difference, e.g. Δv change in velocity	dep.	dep.
ϵ_k	Normalized Estimation Error Squared	-	1
Γ	The input-to-state transition matrix	dep.	dep.
Υ	The noise-to-state transition matrix	dep.	dep.
Φ	The state transition matrix	dep.	dep.
π	Camera plane	n.a.	n.a.
Ψ	Plane defined by Impactor momentum direction and the lever arm w.r.t NEO CoM	n.a.	n.a.
ρ	Correlation coefficient	-	1
ρ_{sc}	Reconnaisance S/C Range Measurement	m	1
$ \rho_{sc} $	Reconnaisance S/C Doppler Measurement	m/s	1
$J\lambda_{sc}$	Reconnaisance S/C Azimuth Measurement	rad	1
$J\epsilon_{neo}$	Reconnaisance S/C Elevation Measurement	rad	1
ρ_{neo}	Pseudo NEO Range measurement	m	1

$ \rho_{neo} $	Pseudo NEO Doppler measurement	m/s	1
$J\epsilon_{sc}$	Pseudo NEO Azimuth measurement	rad	1
$J\epsilon_{neo}$	Pseudo NEO Elevation measurement	rad	1
σ	Standard deviation of Gaussian distr.	dep.	1
σ^2	Variation of Gaussian distribution	dep.	1
μ_x	Mean of Gaussian distribution X	dep.	1
μ	Gravitational parameter	m^3/s^2	1

Math Operators

Symbol	Description
.	Dot product
$E\{\cdot\}$	Expected value operator
T	Transpose operator
Tr	Trace operator
∇	Gradient
\times	Cross-product